

**MYCRO-PHYSICAL APPROACH TO COUPLED
AUTOGENOUS AND DRYING SHRINKAGE OF CONCRETE**

(Translation from Proceedings of JSCE, No.578/V-37, November 1997)



Tetsuya ISHIDA



Rajesh P. CHAUBE



Toshiharu KISHI



Koichi MAEKAWA

The autogenous and drying shrinkage model proposed here is derived from micro-mechanical physics of water in the pore structure of concrete. In the model, the shrinkage of concrete due to self-desiccation, known as autogenous shrinkage, is idealized as being driven by surface tension due to capillary formation of a curved meniscus, similar to the drying shrinkage processes. The overall material properties of concrete are evaluated considering the inter-relationships among the hydration, moisture transport, and pore-structure development processes based on fundamental thermo-physical models. By implementing the shrinkage model, the volumetric changes of concrete can be satisfactorily predicted for different water to cement ratio, curing and mix proportions.

Keywords: *Autogenous shrinkage, capillary tension, drying shrinkage, hydration, pore structure, water content*

Tetsuya Ishida is an assistant lecturer in the Department of Civil Engineering at University of Tokyo, Japan. He obtained his D.Eng from University of Tokyo in 1999. His research interests cover mass/energy transport phenomena in concrete and the mechanisms of shrinkage and creep of concrete. He is a member of the JSCE and the JCI.

Rajesh P. Chaube is a system engineer at Gulf Net Communications Corporation, Tokyo, Japan. He obtained his D.Eng. from University of Tokyo in 1996. His research interests include numerical simulations of concrete performance, development and planning of network softwares.

Toshiharu Kishi is a lecturer in the Department of Structural Engineering at Asian Institute of Technology, Thailand. He obtained his D.Eng. from University of Tokyo in 1996. His research interests include the mechanisms of hydration process of cement in concrete, and thermal stresses in massive concrete. He is a member of the JSCE and the JCI.

Koichi Maekawa serves as professor in the Department of Civil Engineering at the University of Tokyo, Japan. He obtained his D.Eng. from University of Tokyo in 1985. He specializes in nonlinear mechanics and constitutive laws of reinforced concrete, seismic analysis of structures, and concrete thermodynamics. He is a member of the JSCE and the JCI.

1. INTRODUCTION

Self-compacting high performance concrete (HPC)[1] can overcome a number of uncertainties inherent in construction methods (especially concreting works) and produces a reliable structural concrete with high durability. Owing to the requirements of super fluidity and segregation resistance of self-compacting HPC, specifications usually include a small amount of free water and low water to powder ratio. With such a concrete, however, it has been reported that considerable autogenous shrinkage occurs, and that the volume change due to autogenous shrinkage, which can be ignored in the case of ordinary concrete, should be considered in carrying out crack control or durability checking of RC structures [2].

In the hydration process of cementitious powder materials, the total volume of hydrate products will be smaller than the sum of the volumes of unhydrated powder materials and free water for hydration. Therefore, the pore space in hydrated cement paste cannot be full of liquid water, and the relative humidity in pore structures decreases as hydration proceeds. This phenomenon is known as self-desiccation and leads to the autogenous shrinkage of concrete [2].

Past research has often introduced capillary tension theory to explain drying shrinkage behavior [2][5]. Under this assumption, the volume change and deformation of cement paste occurs due to the surface tension force of capillary water across a curved meniscus. In this paper also, it is assumed that capillary tension force caused by a drop in relative humidity in pore structures leads to shrinkage stress, and also that this mechanism causes autogenous shrinkage, as well as the shrinkage caused by concrete drying associated with water migration. As for the constitutive law describing the stress-strain relationship in terms of shrinkage behavior, the model proposed by Shimomura's research was in principle applied in this study [5]. Here, shrinkage stress is determined by pore pressure, pore distribution, and the water content of the hydrated cement paste. The deformability of the microstructure in response to shrinkage stress is modeled based on the computationally evaluated porosity of hydrated cement paste. These material properties of early-age concrete are evaluated by the analytical method coded **DuCOM** considering the inter-relationship of hydration, moisture transport, and the micro-pore structure development process [3]. In this system, autogenous shrinkage need not be distinguished from drying shrinkage caused by water loss. By the proposed system, the authors attempt to predict the volume change of concrete in a unified manner for arbitrary atmospheric conditions.

2. ANALYTICAL MODEL

2.1 Pore structure development [3]

As a physical basis for pore-structure development computations at an early stage of hydration, the overall pore-space is broadly divided into areas with interlayer, gel, and capillary porosity. The powder material is idealized as uniformly sized spherical particles of the same radius. After contact with water, these particles start to dissolve and reaction products are precipitated. Figure 1 shows a schematic representation of the various phases at any arbitrary stage of hydration. Precipitation in the pore solution phase and on the outer surface of the particle leads to the formation of the outer products whereas the inner products are formed inside the original particle boundary where the hydration characteristics are more or less uniform.

Inner product porosity and properties are assumed to be constant throughout the process of pore structure formation. It is assumed that conventional capillary porosity is predominant in the outer products whereas CSH hydrate crystals account for gel and interlayer porosity. The characteristic porosity of the CSH mass ϕ_{ch} is assumed to be constant throughout the hydration process. In this study, a value of 0.28 is assumed [4]. It should be noted that this porosity includes both the interlayer as well as micro-gel porosity.

With these assumptions, the weight W_g and volume V_g of gel solids can be computed, provided the average degree of hydration α and the amount of chemically combined water β per unit weight of powder material are known. These two parameters are obtained from the multi-component hydration heat model. As reported by past researchers, a layer structure for the CSH mass is assumed with an interlayer spacing of one water molecule [14]. The total volume of hydration

products would be less than the summation of unhydrated powder and water volume. In this paper, this volume change during hydration is accounted for by changing the water density for the sake of analytical convenience; that is, the density of free water ρ_L is 1.0 whereas the density of combined water ρ_w is assumed to be 1.25[4]. The overall volume balance thus gives interlayer (ϕ_l), gel (ϕ_g) and capillary (ϕ_c) porosity. These parameters are computed as

$$\phi_l = \frac{t_w s_l \rho_s}{2} \quad \phi_c = 1 - V_s - (1 - \alpha) \frac{W_p}{\rho_p} \quad (1)$$

$$\phi_g = \phi_{ch} V_s - \phi_l \quad V_s = \frac{\alpha W_p}{1 - \phi_{ch}} \left(\frac{1}{\rho_p} + \frac{\beta}{\rho_w} \right) \quad (2)$$

where, t_w : interlayer thickness(2.8Å), s_l : specific surface area of interlayer, W_p : weight of the powder materials per unit volume, ρ_p : density of the powder material, ρ_s : dry density of solid crystals= $(1+\beta)(1-\phi_{ch})/(\rho^{-1}+\beta\rho_w^{-1})$. ϕ_{ch} is the gel particle's porosity and a value of 0.28 is assumed.

The outer products of thickness δ_m are computed by assuming a bulk porosity variation which increases from the characteristics porosity of the solid mass ϕ_{ch} at the particle surface to ϕ_u at the external boundary of the outer products. The parameter ϕ_u equals unity before the expanding cluster reaches the outermost end of the representative spherical cell of the particle. From these parameters, the surface areas of capillary and gel pores can be computed.

In the computational model a bi-model $R-R$ porosity distribution $\phi(r)$ which gives the total porosity function is assumed [3][5]. Thus, we have,

$$\phi(r) = \phi_l + \phi_g V_g(r) + \phi_c V_c(r) \quad (3)$$

where, r : pore radius. $V_g(r)$ and $V_c(r)$ represent the fractional pore volumes of gel and capillary pores in the distribution, respectively (Fig.2).

$$V_i(r) = 1 - \exp(-B_i r) \quad (0 \leq V_i(r) \leq 1) \quad (4)$$

$$dV_i = B_i r \exp(-B_i r) d \ln r \quad (5)$$

Distribution parameters B_i represent the peak of the porosity distribution on a logarithmic scale. If we assume a cylindrical pore shape in such a distribution, these parameters can be easily obtained from the computed porosity and surface area values for the capillary and micro-gel regions.

2.2 Multi-component hydration model [6]

a) Thermodynamic equilibrium of liquid and vapor phases

The hydration process is simulated by using multi-component model for heat of hydration of cement proposed by *Kishi et al.* Specified chemical components of clinker minerals are treated as the characteristic parameter and the influence of variable moisture content and powder material

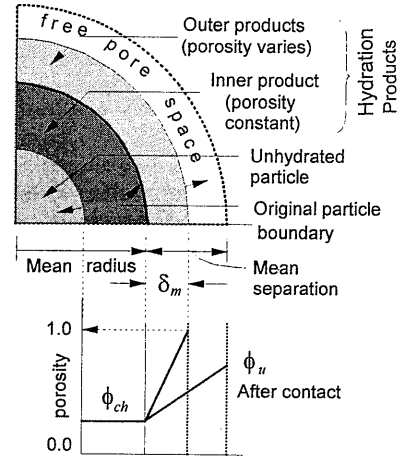


Fig.1 Micro pore-structure development model

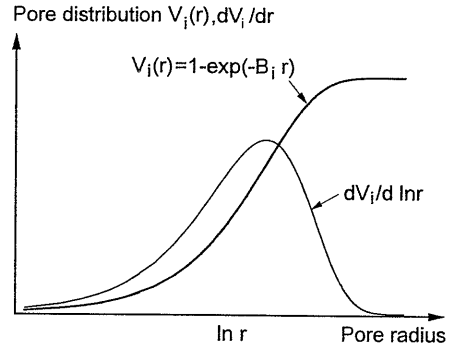


Fig.2 Definition of the porosity distribution function

where, P_v/P_w : relative humidity of vapor phase, γ : surface tension of liquid water [N/m], M_w : molecular mass of water [kg/mol], R : universal gas constant [J/mol·K], T : absolute temperature [K], ρ_L : density of liquid water [kg/m³], r_s : the radius of the pore in which the interface is created [m]. Due to the surface tension of liquid water, the pressures of gas and liquid are not equal. This pressure difference ΔP would be described by Laplace's equation as,

$$\Delta P = P_G - P_L = \frac{2\gamma}{r_s} \quad (9)$$

where, P_G, P_L : pressure of gas and liquid phase respectively [Pa]. The pressure of each phase can be computed by moisture isotherm and transport model. From eq. 9, we can clarify that the pressure of the liquid phase is lower than that of the gas phase, and tensile stress would act on pore walls where there is contact with the liquid phase. In this paper, the volume change at a microscopic level due to this stress is assumed to cause both autogenous shrinkage and drying shrinkage on the macroscopic scale. The total intensity of tensile stress per unit concrete volume will depend on both the magnitude of the tension and the area where it is applied. We adopt Shimomura's formulation for the capillary stress that causes drying shrinkage as [5],

$$\sigma_s = A_s \frac{2\gamma}{r_s} \quad (10)$$

where, σ_s : capillary stress [Pa], A_s : area factor [m³/m³]. The capillary stress acts on pore walls where liquid water exists. Therefore, in this paper, A_s is defined as the total liquid water content per unit concrete volume, and it can be obtained from hysteretic isotherms, moisture transport, and the pore structure development model. The stress-strain relationship, which describes the micro deformation of cement paste due to capillary stress, might be nonlinear. However, at this stage it is difficult to take account of the nonlinear behavior of C-S-H crystals at micro level. In this study, using the elastic modulus for capillary stress E_s , which includes various aspects of nonlinear deformational behavior, the stress-strain relationship is assumed as [5]

$$\varepsilon_{sh} = \frac{\sigma_s}{E_s} \quad (11)$$

where, ε_{sh} is the unrestrained macroscopic shrinkage strain.

3. ANALYTICAL STUDY OF SHRINKAGE BEHAVIOR WITH THE PROPOSED MODEL

3.1 Outline of computational scheme for solving material properties

An analytical study of the autogenous and drying shrinkage behavior of mortar and concrete was carried out using the proposed shrinkage model. To treat both autogenous, drying behavior and their coupling in the same scheme, the various material properties, namely, hydration, pore-structure development, moisture distribution, relative humidity in pores, and the deformability for capillary stress should be predicted with time and space. In this study, to verify the shrinkage behavior of concrete for arbitrary mix proportions, curing conditions, and environmental conditions, the proposed shrinkage model was implemented in the finite-element computational program **DuCOM** [3].

An outline of the overall computational scheme is shown Fig.3. The inputs required are mix proportion, powder material characteristics, casting temperature, the geometry of the target structure, and the boundary conditions to which the structure will be exposed during its life cycle. First of all, using the multi-component hydration model, solutions to the temperature, degree of hydration, and amount of chemically combined water are obtained. Once this information related to the hydration process is obtained, the geometry of the pores is determined by the pore structure development model. The resulting porosity and pore distributions are used to evaluate moisture conductivity. Using the moisture transport model, which considers both vapor and liquid transports, the pore pressure, relative humidity, and moisture distribution can be obtained. In

proportions in the mix is taken into consideration. Total heat generation rate H per unit volume is described as eq. 6.

$$H = C \sum p_i H_i \quad H_i = H_{i,T_0} \exp \left[-\frac{E_i}{R} \left(\frac{1}{T} - \frac{1}{T_0} \right) \right] \quad (6)$$

where, C : the cement content per unit volume, p_i : corresponding mass ratio in the cement, H_i : the specific heat generation rate of an individual clinker component, computed using Arrhenius's law, E_i : activation energy of the i -th component, R : gas constant, H_{i,T_0} : the referential heat rate of i -th component when temperature is T_0 . The referential heat rate of each reaction embodies the probability of molecular collisions by which hydration proceeds. In this model, it is taken as a function of the amount of free water, the thickness of the cluster already formed by the hydrated products and unhydrated chemical compounds, and the total accumulated heat of each clinker component. The total amount of free water in the model is in fact the total condensed water in the micro-pore structure, which is obtained by moisture isotherm and transportation model, and pore structure development model.

In the above hydration model, the average degree of hydration α and the chemically combined water β per unit weight of powder material are obtained for an arbitrary stage of hydration. These parameters are essential for describing the pore structure development process, and the total amount of water consumed per unit volume of concrete due to hydration is dynamically coupled with the overall moisture balance.

2.3 Moisture transport formulation [7][8][9]

The ingress of moisture into the pores of concrete is a thermodynamic process driven by pressure and temperature potential gradients. In this study, the total water present in matrix pores is categorized as interlayer, adsorbed, and condensed water. Interlayer water is water which is most likely under the influence of strong surface forces and which perhaps does not move under the influence of pore pressure potential gradients. The absorption-desorption characteristic of the interlayer water is modeled based on the Feldman and Sereda interlayer model [14]. The amount of water dispersed in the remaining microstructure as condensed and adsorbed phases is obtained by integrating the degree of saturation of individual pores, considering local thermodynamical equilibrium and modified B.E.T. theory [7]. Furthermore, the hysteresis behavior, by which the water content of concrete differs in the drying and wetting processes, is described by considering the geometrical characteristics of random pore structures [9]. The overall moisture balance, which also takes into account the consumption of water during early-age hydration, can be obtained as

$$\rho_L \left(\sum \phi_i \frac{\partial S_i}{\partial P_L} \right) \frac{\partial P_L}{\partial t} - \text{div}(K(P_L, T) \nabla P_L) + \rho_L \sum S_i \frac{\partial \phi_i}{\partial t} - W_p \frac{\partial \beta}{\partial t} = 0 \quad (7)$$

where, ϕ_i : porosity of each component (interlayer, gel, and capillary), S_i : degree of saturation of each component, P_L : equivalent liquid pore pressure, ρ_L : density of pore water. The moisture conductivity K is obtained from the flux models proposed by *Chaube et al* using the computed R - R distribution function [8].

2.4 Autogenous and drying shrinkage model based on micromechanism [5]

The relative humidity in the pore structure decreases with drying due to the RH gradient between ambient conditions and the interior concrete, or by self-desiccation even if egress of moisture to the outside does not occur. Considering local thermodynamic and interface equilibrium, vapor and liquid interfaces would be formed in the pore structure due to the pressure differences caused by capillarity. Where the interface is a part of an ideal spherical surface, this relation can be described by Kelvin's equation as

$$\ln \frac{P_v}{P_{vo}} = -\frac{2\gamma M_w}{RT\rho_L r_s} \quad (8)$$

calculating the pore pressure, the governing equation is the mass balance of moisture and this should be satisfied. In this scheme, the moisture consumed by the hydration process is included in the mass balance equation. This inter-dependency makes it possible to couple the early-age hydration problem dynamically, and also makes it possible to consider the hydration process under any curing and environmental conditions. Based on the above, **DuCOM** gives solutions for the various material properties in 3D space and the time domain.

In this computational system, it is not necessary to distinguish the behavior of autogenous and drying shrinkage behavior. By calculating the water content and pore structure of the concrete under given initial environmental and curing conditions, we can predict the volume change due to shrinkage behavior from eq. (11).

This 3D FE program **DuCOM** is accessible on the WWW at the address <http://concrete.t.u-tokyo.ac.jp/en/demos/ducom/index.html>, and anyone can obtain analytical solutions, though the dimension and the number of elements of the target structure is limited.

3.2 Analysis of the shrinkage behavior

For verification, prismatic specimens were used. In this case, based on the assumption of a uniform deformation in one direction, the shrinkage of the specimen can be calculated as the average of the free unrestrained shrinkage strain. It has to be noted that the free shrinkage strain would be different with each finite element, because this calculated value is dependent on the moisture content, pore pressure, micro-pore structure, and hydration level. Consequently, it is also possible to predict the internal stress of a restricted structural member by combining this model with a structural analysis program.

In this computational scheme, for a given pore pressure and total water content in the pores as calculated by **DuCOM**, the capillary stress σ_s can be obtained from eq. (10). As for E_s , which indicates the deformability against the capillary stress, it has been reported from past research that E_s is about 1/3-1/4 of the ordinary value of static elastic modulus E_c of concrete under extensive stress at a higher than actual loading rate [5]. In this paper, also, there is some relationship between E_s and E_c , and in all cases E_s is assumed to be 1/4 of E_c . The effect of creep behavior might be included in E_s . It has also reported that a good correlation between E_c and the compressive strength of concrete exists [4][10]. Therefore, to obtain the elastic modulus E_c , we will attempt to estimate the compressive strength from the porosity of hydrated cement paste as

$$f'_c = A \exp(-B \cdot V_{pore}) \quad (12)$$

where, f'_c : compressive strength[Pa], V_{pore} : pore volume per unit paste volume[m³/m³], A, B : constant. In general, it has been reported that compressive strength is dependent on the pore volume of the cement paste, especially, when it comprises radii in the 50nm -2 μ m range [10]. Therefore, the total volume of pores of radii above 50nm is assumed to be V_{pore} in eq. (12). Using **DuCOM**, V_{pore} can be analytically obtained from the solutions to the porosity and pore distribution of the capillary in each element over time.

$$V_{pore} = \phi_c \cdot \exp(-B_c \cdot r) \quad (13)$$

where, ϕ_c is capillary porosity, B_c is the distribution parameter for capillary pore, and r is 5.0×10^{-8} [m].

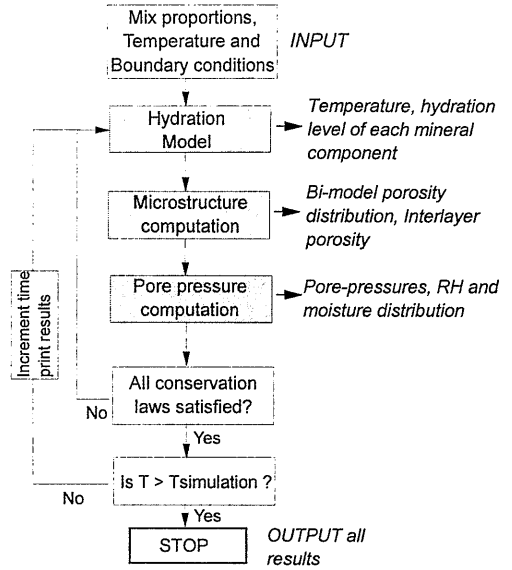


Fig.3 Coupled 3D-FEM scheme of solution for hydration, moisture transport, and structure formation problem in concrete

Figure 4 shows the relationship between measured compressive strength and computed capillary porosity (above 50nm). The 38 specimens of mortar and concrete in Fig.4 were tested under various conditions; that is, water to cement ratio by weight: 24-51%; the aggregate volume: 40%-65%; type of powder materials: ordinary, medium heat and high-belite cement, blast furnace slag; curing conditions: sealed, submerged and exposed curing; curing temperature: 20°C, various temperature histories; age of specimen: 0.5-28 days. To compute the capillary porosity of each test specimen, the same conditions were used as in the experimental analysis. The computed porosity obtained by **DuCOM** involves the effects of age, curing conditions, temperature, and mix proportion.

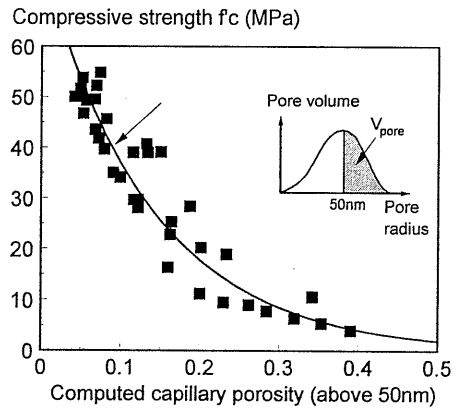


Fig.4 Relationship between measured compressive strength and computed capillary porosity

It has been discovered that the compressive strength of mortar and concrete depends on the strength of the aggregate and the transition zone between aggregate and cement paste matrix, as well as the porosity of the cement paste. In this research, these factors are assumed to be negligible, since a low water to powder ratio is specified in the mix proportions and natural aggregates of low porosity are used for all test specimens

The above relationship between compressive strength and computed porosity was regressed with an exponential function, and the constants A and B in eq. (12) were obtained. The elastic modulus of concrete E_c was calculated from empirical formula [11] and the compressive strength relationship of eq. (12). As already mentioned, deformability against capillary stress E_c is assumed to be $1/4$ of E_c in this analysis.

3.3 Verifications

3.3.1 Drying shrinkage behavior

The powder materials, mix proportions, specimen size, and experimental conditions used in this test are shown in Table 1. The target here is to verify the moisture loss and drying shrinkage behavior of the mortar (No.1, 2 in Table1). In the experiment, the water to powder ratio was 28% and the mortar specimens were $4 \times 4 \times 16$ [cm]. After 2 days of sealed curing, the specimens were exposed to drying at 66%RH, and 45%RH at 20°C, and moisture loss and length change with time were measured. In the FEM analysis, mix proportions and the chemical composition of the cements (C_3A , C_4AF , C_3S , C_2S , and gypsum) were given. The curing conditions and exposure conditions were also given as boundary conditions for the target structures. All of these input values corresponded to the experimental conditions. In the tests, drying started after 2 days of sealed curing, as noted. The mesh for FE analysis is shown in Fig.5. This analysis implicitly takes into account the effects of autogenous shrinkage even under drying conditions, while hydration could still be significant. Of course, the effect of delayed hydration due to a loss of free water under drying conditions can be coherently evaluated by the analysis. The computed results of moisture loss and shrinkage behavior show reasonable agreement with the experimental data (Figs. 6,7).

3.3.2 Autogenous and drying shrinkage of mortar and concrete

The second case is the study of volume change due to both autogenous and drying shrinkage of mortar and concrete. As already mentioned, within the framework of analysis by **DuCOM**, the volume change can be predicted based on micro mechanisms considering capillary tension force in a pore. No matter how the capillary tension is caused, by moisture loss due to drying or by a self-desiccation, coupled autogenous and drying shrinkage behavior can be obtained by calculating the pore structure, the RH in pores, water content and deformability at each element over the time domain.

Table.1 Experimental conditions of test specimens

Specimen No.	Powder materia l	W/C (%)	Volume of Aggregate	Specimen size [cm]	Drying conditions
1 (Mortar)	MC* ¹	28%	50%	4×4×16	66%RH after 2 days
2 (Mortar)	MC	28%	50%	4×4×16	45%RH after 2 days
3 (Concrete)[12]	OPC* ²	40%	62%	10×10×120	Sealed
4 (Concrete)[12]	OPC	30%	62%	10×10×120	Sealed
5 (Concrete)[12]	OPC	30%	62%	10×10×120	50%RH after 1 day
6 (Mortar)[12]	HS* ³	30%	38%	10×10×40	50%RH after 7 days
7 (Mortar)[12]	HS	30%	38%	10×10×40	Sealed
8 (Mortar)[12]	HS	50%	38%	10×10×40	50%RH after 7 days
9 (Mortar)[12]	HS	50%	38%	10×10×40	Sealed
10 (Mortar)	OPC	25%	50%	4×4×16	60%RH after 7 days
11 (Mortar)	OPC	25%	50%	4×4×16	60%RH after 28 days
12 (Mortar)	OPC	55%	50%	4×4×16	60%RH after 28 days

*1: Medium heat cement, *2: Ordinary portland cement, *3: High-strength cement.

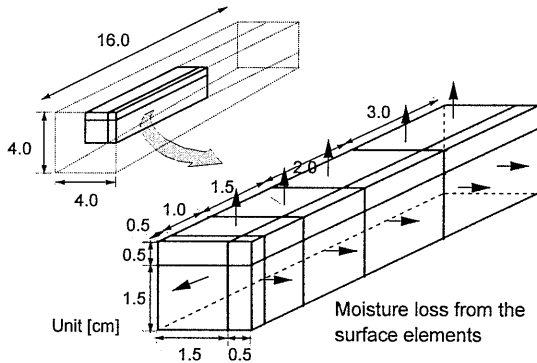


Fig.5 Mesh layout used for FE analysis

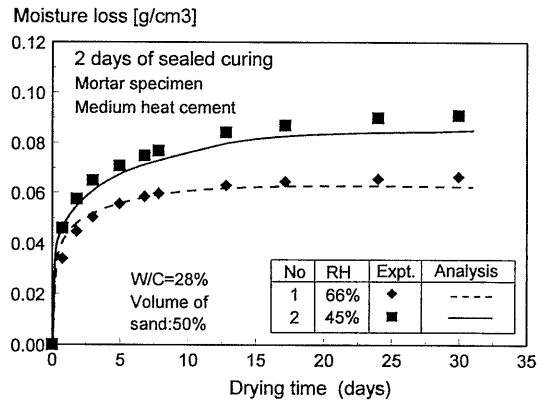


Fig.6 Moisture loss behavior for different drying conditions

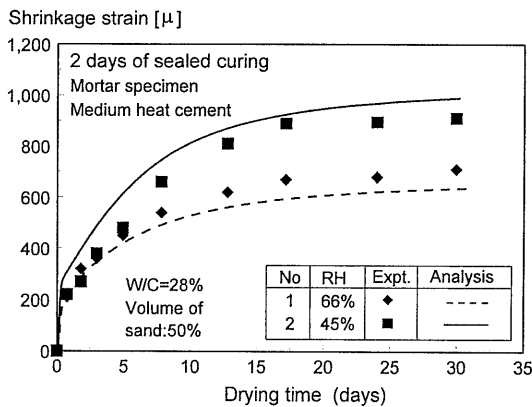


Fig.7 Drying shrinkage behavior for different drying conditions

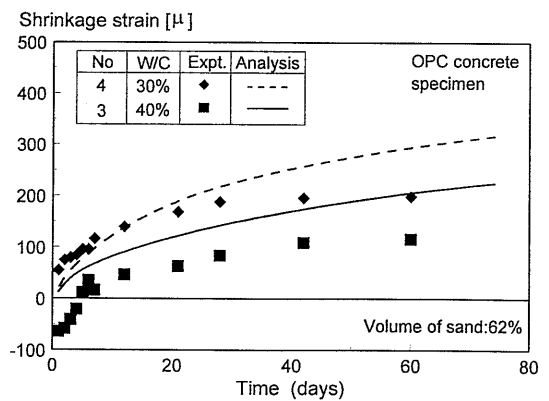


Fig.8 Autogenous shrinkage behavior of concrete for different W/C

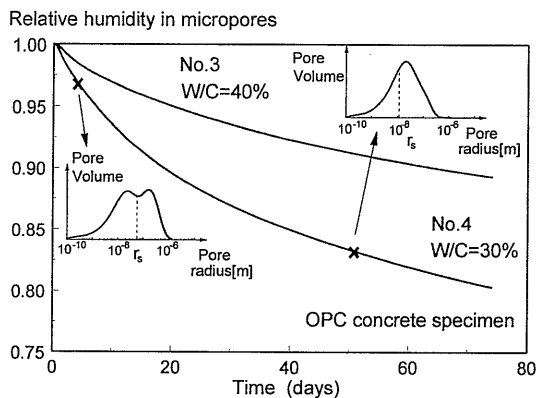


Fig.9 Simulated relative humidity curves in pore structure under sealed conditions

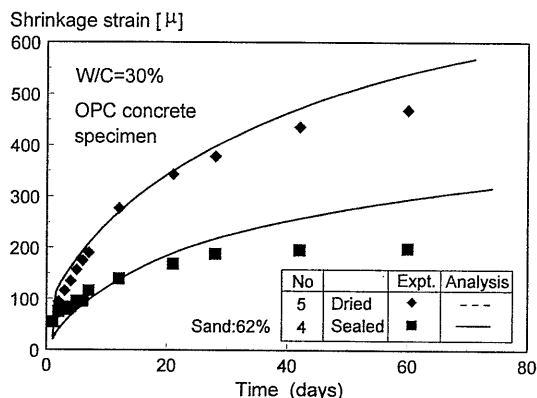


Fig.10 Prediction of autogenous and drying shrinkage behavior of concrete specimen

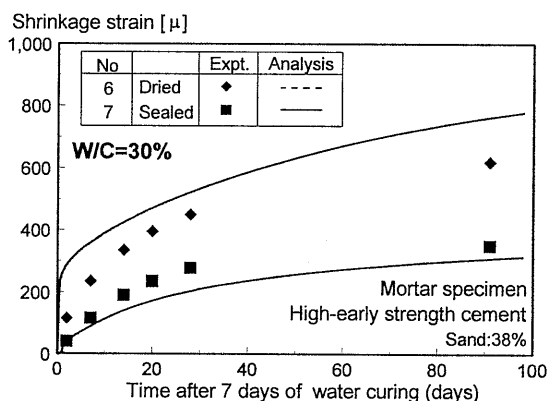


Fig.11 Autogenous and drying shrinkage behavior of mortar (W/C30%)

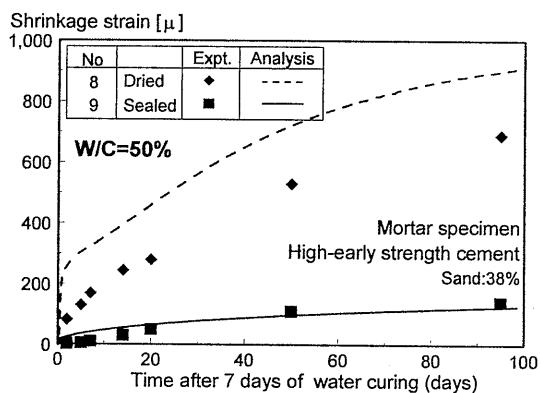


Fig.12 Autogenous and drying shrinkage behavior of mortar (W/C50%)

First, the autogenous shrinkage behavior of concrete was studied. For verification, the experimental data by *Tazawa et al* [12] were used (No.3, 4). The size of mortar specimens was $4 \times 4 \times 16$ [cm], and the volume changes were measured under sealed conditions at 20°C . In this case, the computed RH in pores and the intensity of capillary tension are dependent on the chemically combined water obtained by hydration model and the volume change of hydrated cement paste computed by pore structure formation model, since there is no moisture movement through the boundary element. Figure 8 shows the simulated autogenous shrinkage. The calculation can roughly matches the actual autogenous shrinkage strain for each W/C case. Figure 8 shows the analytically predicted average RH in the pore structure of the concrete, the porosity distribution, and the radius of the pore r_s in which an interface between liquid and vapor is created (eq.(8)). As shown in Fig.9, the average radius of pores in hydrated cement paste decreases as hydration proceeds. At the same time, the free water for hydration is consumed. This results in a depletion of liquid water in the pores. In Fig.9, this space would occupy the pores whose radii are above r_s . In **DuCOM**, considering the thermodynamic equilibrium condition, RH in vacant pore space can be obtained from this radius r_s and the surface tension of the liquid. The calculated value of RH decreases with time. For W/C 40% and 30%, the pore humidity decreases to 90% and 80%, respectively. This result appears rational, since past research [13] has reported a similar quantitative trend in the decrease of pore with time. The drop in RH causes a surface tension force, and autogenous shrinkage can be obtained numerically.

Next, the authors verified combined autogenous and drying shrinkage in a test on mortar and concrete specimens, with similar mix proportions and curing conditions (Specimen No. 4-9). The

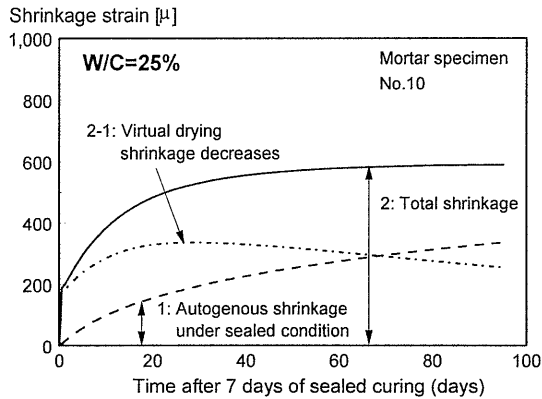


Fig.13 Nonlinearity of autogenous and drying shrinkage behavior

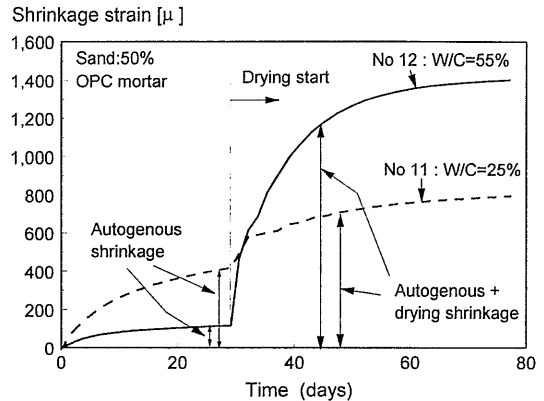


Fig.14 Numerical simulation of autogenous and drying shrinkage behavior for different water to cement ratio

one specimen was kept sealed, and the other was dried under 60% RH (Fig.10), 50%RH (Fig. 11, 12) after a certain curing period. The analytical results show good agreement with the experimental data for different materials, mix proportions, and curing conditions in terms of both autogenous and drying shrinkage.

3.3.3 Numerical simulation of coupled autogenous and drying shrinkage

Using the proposed system, several numerical sensitivity simulations to demonstrate the behavior of autogenous and drying shrinkage were implemented.

The first case is a study of the nonlinearity of autogenous and drying shrinkage behavior. Figure 13 shows the computational results of mortar shrinkage behavior, when exposed to drying after 7 days of sealed curing (Specimen No.10). In Fig.13, solid line 2 indicates total shrinkage strain, whereas dotted line 1 shows autogenous shrinkage strain under perfectly sealed condition. If total shrinkage strain can be assumed to be the linear summation of autogenous shrinkage under sealed condition and drying shrinkage, the contribution of drying shrinkage would be the difference between total shrinkage and autogenous shrinkage, that is line 2-1 in Fig.13. As a result, this virtual drying shrinkage strain 2-1 decreases under the assumption that linear summation is correct. In fact, under drying conditions, the autogenous shrinkage would be less than that under sealed conditions, because of the delay in hydration due to moisture loss to the outside. Without considering this aspect, the contribution of autogenous shrinkage would be overestimated. Namely, in predicting actual shrinkage behavior, it is necessary to consider the interdependence between moisture loss and the hydration process.

The second case considers numerical simulations for quite different W/C ratios (Fig.14). The case of W/C 55% was analyzed as ordinary concrete, whereas that of W/C 25% as self-compacting concrete or high-strength concrete (No.10, 11, Table1). The specimen was exposed to RH 60% drying condition after 28 days of sealed curing. It has been reported that the shrinkage behavior of ordinary concrete is quite different from that of low W/C ratio concrete [2]. In the case of ordinary concrete, the contribution of autogenous shrinkage to the total volume change is relatively small compared with the drying shrinkage contribution. On the other hand, in the case of low W/C concrete, the effect of autogenous shrinkage is not negligible compared with drying shrinkage. The analytical results accurately reflect this qualitative tendency.

4. CONCLUSIONS

A micro-physical model for the autogenous and drying shrinkage of concrete based on micro mechanical approach is presented in this paper. Capillary stress was assumed to cause autogenous shrinkage and drying shrinkage. The material properties of young concrete were obtained by

coupled analysis considering the inter-relationships among the hydration, moisture transport, and pore-structure development processes. This framework offers a prediction method for the volume change of concrete due to autogenous, drying shrinkage and their combination for arbitrary mix proportions, materials, ages, curing conditions, and environmental conditions. The entire scheme is expected to form the basis of future a performance-based durability design.

Acknowledgement

The authors wish to thank Professor Hajime OKAMURA (University of Tokyo) and Associate Professor Takumi SHIMOMURA (Nagaoka University of Technology) for their valuable suggestions during the course of this study.

References

- [1] Okamura, H., Maekawa, K. and Ozawa, K.: *High Performance Concrete*, Gihodo, Tokyo, 1993 (In Japanese).
- [2] JCI: *The report of JCI Committee on Autogenous Shrinkage*, 1996.
- [3] Maekawa, K., Chaube, R.P. and Kishi T.: Coupled mass transport, hydration and structure formation theory for durability design of concrete structures, *Proc. of the Int'nl workshop on rational design of concrete structures under severe conditions*, Hakodate, pp. 263-274, 1995.
- [4] Neville, A.M.: *Properties of Concrete*, ISMN, London, 1979.
- [5] Shimomura, T. and Maekawa, K.: Analysis of the drying shrinkage behavior of concrete using a micromechanical model based on the micropore structure of concrete, *Concrete Library of JSCE*, No.27, pp. 121-143, 1996.
- [6] Kishi, T. and Maekawa, K.: Multi-component model for hydration heating of portland cement, *Concrete Library of JSCE*, No.28, pp.97-115, 1995.
- [7] Chaube, R.P. and Maekawa, K.: A study of the moisture transport process in concrete as a composite material, *Proceedings of the JCI*, Vol. 16, No.1, pp.895-900, 1994.
- [8] Chaube, R.P. and Maekawa, K.: A permeability model of concrete considering its microstructural characteristics, *Proceedings of the JCI*, Vol. 18, No.1, pp. 927-932, 1996.
- [9] Ishida, T., Chaube, R.P., Kishi, T. and Maekawa, K.: Modeling of pore water content in concrete under generic drying wetting conditions, *Concrete Library of JSCE*, No.31, pp.275-287, 1998.
- [10] Uchikawa, H., Uchida, S. and Hanehara, S.: Advances in cement manufacture and use, Engineering foundation conference, pp.271-294, 1988.
- [11] Okamura, H. and Maeda, S: *Reinforced Concrete Engineering*, Ichigaya Syuppan, Tokyo, 1987 (In Japanese).
- [12] Tazawa, E. and Miyazawa, S.: Influence of binder and mix proportion on autogenous shrinkage of cementitious materials, *Proc. of JSCE*, No.502, V-25, pp.43-52, 1994 (in Japanese).
- [13] Paille, A.M., Buil, M. and Serrano, J.J.: Effect of fiber addition on the autogenous shrinkage of silica fume concrete, *ACI Material Journal*, Vol.86, No.2, pp.139-144, 1990.
- [14] Feldman, R.F. and Sereda, P.J.: A model for hydrated portland cement paste as deduced from sorption-length change and mechanical properties, *Master. Constr.*, Vol.1, 509-519, 1968.